Macromolecules
PERSPECTIVE

Macromolecules **2010**, *43*, 5163–5176 **5163**
DOI: 10.1021/ma1006396

Exploitation of Intrinsic Microporosity in Polymer-Based Materials

Neil B. McKeown*,† and Peter M. Budd*,‡

†*School of Chemistry, Cardiff University, Cardiff CF10 3AT, U.K., and* ‡*School of Chemistry, The University of Manchester, Manchester M13 9PL, U.K.*

Received March 23, 2010; Revised Manuscript Received April 30, 2010

ABSTRACT: The past decade has seen the development of microporous materials (i.e., materials containing pores of dimensions < 2 nm) derived wholly from organic components. Here we review this nascent area with a particular emphasis on amorphous polymers that possess intrinsic microporosity (IM), which is defined as microporosity that arises directly from the shape and rigidity of component macromolecules. Although IM can be readily identified within soluble non-network polymers and oligomers, for network polymers it is harder to differentiate IM from template effects that are responsible for the microporosity within hyper-cross-linked networks. The numerous examples of microporous polymers assembled from rigid monomers by the formation of rigid linking groups are surveyed and their IM assessed. The potential applications of these materials are highlighted.

Introduction

Microporous materials are solids containing interconnected pores of less than 2 nm in size that can be exploited for heterogeneous catalysis, adsorption, separation, and gas storage.[1] Conventional microporous materials consist of crystalline inorganic frameworks (e.g., zeolites and related structures) or amorphous network structures (e.g., silica, activated carbon). However, the past decade has seen major advances in the preparation of microporous materials using organic components. For example, great interest has been generated by crystalline organic−inorganic hybrid materials, such as Yaghi's metal organic frameworks (MOFs)[2−4] and the structurally related purely organic covalent organic frameworks (COFs).[5,6] These porous crystals are assembled under thermodynamic control using rapidly reversible bonding and hence favor the formation of the most stable structure. Generally, porous materials are less stable than those that are densely packed, but in the case of MOFs and COFs the void space within the crystal structure is initially filled with solvent molecules, which are removed by the application of heat and vacuum after synthesis. The breakthrough property of these materials, as compared to previously obtained open-framework coordination polymers,[7] is that the ordered structure of the framework is maintained during solvent evacuation to provide what is often called "permanent" porosity, as demonstrated by reversible gas adsorption (e.g., N_2 at 77 K). In low-temperature N_2 adsorption, microporous materials are characterized by high uptake at very low relative pressures and by high apparent surface areas as determined, typically, by the Brunauer−Emmet−Teller (BET) method.[8]

Commercially useful amorphous materials, such as activated carbons, demonstrate that crystalline order is not a prerequisite for microporosity, and it was established more than 30 years ago that amorphous organic microporous materials can be prepared by the formation of a hyper-cross-linked polymer (HCP) network.[9,10] Such materials are assembled under kinetic control using irreversible polymerization reactions, for example, by the cross-linking of chloromethylated styrene using Friedel−Crafts alkylation, and are obtained initially as solvent-swollen gels.[11,12] Over the past decade a great variety of hyper-crosss-linked microporous polymer networks have been prepared using different polymerization chemistries and monomers.[9,10,13−19] On removal of the solvent, HPCs display permanent porosity (e.g., apparent BET surface areas up to 2000 $m^2\ g^{-1}$)[12,14] with a broad pore size distribution ranging from micropores through mesopores (2−50 nm) to macropores (> 50 nm).[11] The microporosity within HPCs can be thought to arise from the template effect of the solvent molecules trapped within the polymer network as it forms, whereas the larger pores originate from phase separation of the polymer from the solvent. The mechanism of micropore formation within HPCs appears closely related to that which occurs to give molecularly imprinted polymers (MIPs), in which a highly cross-linked network is prepared around template molecules of interest, so that when the template is removed a receptor site of the correct size, shape, and binding functionality is obtained.[20] Therefore, the microporosity in MIPs and HCPs could be described as "extrinsic" with the relatively soft polymer matrix being molded around a rigid template.

In recent years we have prepared amorphous organic microporous materials by exploiting the concept of intrinsic microporosity (IM),[21−37] defined as "a continuous network of interconnected intermolecular voids, which forms as a direct consequence of the shape and rigidity of the component macromolecules".[38,39] In general, polymers pack space so as to maximize attractive interactions between the constituent macromolecules and, hence, minimize the amount of void space (from a molecule's point of view "empty space is wasted space").[40] Most polymers have sufficient conformational flexibility to allow them to rearrange their shape so as to maximize intermolecular cohesive interactions and pack space efficiently. However, several members of well-established classes of polymers can possess IM (e.g., polyacetylenes, fluorinated polymers, and polyimides), and these are exploited in the polymer membrane field where they are more commonly described as high free volume or ultrapermeable polymers.[41] Our approach to maximizing IM has been to design polymers with highly rigid and contorted molecular structures to provide "awkward" macromolecular shapes that cannot pack space efficiently. These polymers of intrinsic microporosity (PIMs) do not possess rotational freedom along the polymer

*To whom correspondence should be addressed: e-mail mckeownnb@cardiff.ac.uk; Ph +44(0)2920-875851 (N.B.M.); e-mail peter.budd@manchester.ac.uk; Ph +44 (0)161-2754710 (P.M.B.).

Published on Web 05/20/2010

Neil B. McKeown is Professor of Materials Chemistry at Cardiff University. He received his PhD in organic chemistry from the University of East Anglia in 1987. After postdoctoral research at York University (Canada) and the University of Toronto, he obtained his first independent academic post at the University of Manchester in 1991 where he stayed until moving to Cardiff in 2004. His interests span many aspects of organic materials chemistry with particular recent emphasis on the synthesis of nanoporous molecular crystals and microporous polymers. For the latter work he was awarded the 2008 Beilby Medal jointly by the Royal Society of Chemistry, the Society of Chemical Industry, and the Institute of Materials, Minerals and Mining.

Peter M. Budd is a Reader in Chemistry at the University of Manchester. He received his PhD in polymer chemistry from Manchester in 1981. After a period in industry, working as a research chemist at the BP Research Centre in Sunbury-on-Thames, he returned to Manchester as a lecturer in 1989. He is a Fellow of the Royal Society of Chemistry and a member of the American Chemical Society. His research involves the preparation, characterization, properties, and applications of polymers, with particular interests in membrane and adsorption processes for applications such as carbon dioxide capture.

backbone, which ensures that the macromolecular components cannot rearrange their conformation, so that their "awkward shape" is fixed during synthesis. In this Perspective, we discuss further the concept of intrinsic microporosity, indicating synthetic routes to polymer-based microporous materials, discussing how their pore structure may be characterized, and outlining promising avenues for their exploitation.

Structural Requirements for Intrinsic Microporosity

PIMs are polymers with relatively rigid, "awkwardly shaped" backbones. In the context of promoting inefficient packing, can the vague description of an "awkwardly" shaped polymer be more rigorously defined? The mathematical theory of packing 3D geometric shapes into space has had a long history, and it has been calculated that most solid, convex shapes can fill space with a packing efficiency coefficient of at least 0.74,[42,43] which is the optimum value for identical spheres and is similar to the typical packing efficiency of molecules within a crystal.[40,44] The optimal packing efficiency of any shape is an ordered arrangement and random (i.e., amorphous) packing lowers packing coefficients significantly (e.g., that of the most efficient random close packing of spheres is thought to be 0.64).[42] Furthermore, it has been demonstrated by mathematical modeling that random packing of geometric shapes with strongly concave faces is highly inefficient, and this can be explained qualitatively by the incomplete mutual interpenetration of the concavities.[45,46] Hence, we can describe molecules with "awkward" shapes as those that pose similar packing problems due to their concavities. Such molecules have been assigned "internal molecular free volume" (IMFV), as defined by Swager et al.[47] (see Figure 1A), and this concept has been used to explain the physical properties of triptycene-containing polymers[48−53] and liquid crystals,[47,54] which self-assemble by mutual interpenetration of the triptycene units so as to minimize the IMFV arising from the component's three concavities.

The possible solid-state packing arrangements of a typical concave molecular unit, and those of macromolecules prepared by linking them together, are represented in two dimensions in Figure 1. Often, cavity-containing molecules form clathrate crystals with a relatively dense packing arrangement, with solvent molecules filling any residual voids resulting from the IMFV as depicted in Figure 1B. In most cases removal of the solvent results in the collapse of the crystal, however, recent studies have shown that several such molecular crystals (e.g., that of 3,3′,4,4′-tetra-(trimethylsilylethynyl)biphenyl) can possess significant permanent porosity.[55−57] In most cases, random packing of concave-shaped molecules, as represented in Figure 1C, will give an amorphous glass with a larger amount of free volume than the crystal, but for most concave molecules this will be insufficient to provide IM, for which the voids must be sufficiently interconnected for transport of a probe molecule to occur with minimal energy barrier. Figure 1D represents the packing within crystalline COFs for which the porosity is optimized by linking the apexes of the concave units such as triphenylene or tetraphenylmethane using borate ester[5,6] or enamine[58] links to provide crystalline open frameworks. This general strategy of linking concave shapes to produce open crystalline frameworks was previously exploited by Wuest to obtain hydrogen-bonded molecular crystals, with impressively large porosity, which, unfortunately, are unstable to the complete removal of included solvent.[59,60]

Figure 1E−G gives a two-dimensional depiction of IM arising from the random packing of oligomers, polymers, and networks that are derived from linking the apexes of rigid concave molecular units via fused rings or using linking groups within which rotation is severely hindered. Below, we review polymer-based materials that possess IM arising from rigid components with well-defined concavities and attempt to make a conceptual distinction between porosity due to other factors, especially molecular template effects, which are characteristic of hypercross-linked polymers.

Perhaps the clearest demonstration of IM is found for well-defined rigid oligomers containing triptycenes as the concave unit, such as MacLachlen's nickel−salen-linked triptycene oligomers[61] and our organic molecules of intrinsic microporosity[62] (OMIMs, Figure 2). These molecules possess sufficiently large concavities that mutual interpenetration is highly restricted, and they form microporous glasses as represented in Figure 1E. These oligomers can adsorb significant amounts of nitrogen at 77 K and possess apparent BET surface areas of up to 600 $m^2 g^{-1}$. Therefore, an extended macromolecular structure is not necessary for generating solids with IM.

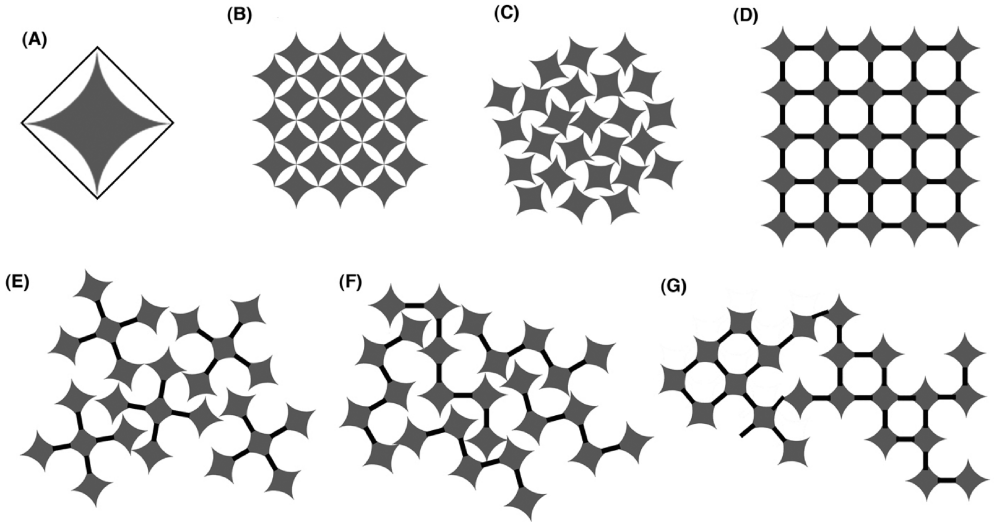

Figure 1. Two-dimensional representations of the solid-state packing of a concave molecular unit (A) shown enclosed within its equivalent nonconcave geometric shape. The internal molecular free volume (IMFV) is defined as the difference in volume of the concave unit as compared to the nonconcave shape and is a measure of concavity. (B) A space-efficient crystal packing arrangement analogous to that found in clathrates. (C) A random packing arrangement for the concave molecular units for which the free volume is greater than the sum of the IMFV of the component units but is not sufficient for microporosity. (D) The least space efficient crystalline packing arrangement obtained by linking the concave units at their apexes to obtain a crystal containing macrocyclic porosity that is much greater than the sum of the IMFV (the black bars indicate bonding). This arrangement is analogous to that found in COFs and related materials. (E) The amorphous packing of well-defined rigid oligomers based on the concave unit (e.g., oligomeric molecules of intrinsic microporosity (OMIMs), Figure 2). Such oligomers possess large concavities for which mutual interpenetration is highly restricted. (F) The amorphous packing of concave units incorporated into non-network polymers of intrinsic microporosity (PIMs). The IP arises from the mutually impenetrable concavities formed due to the contorted shape of the rigid polymers. (G) An amorphous network polymer derived from the concave unit with the IP arising from concavities including those associated with macrocycles.

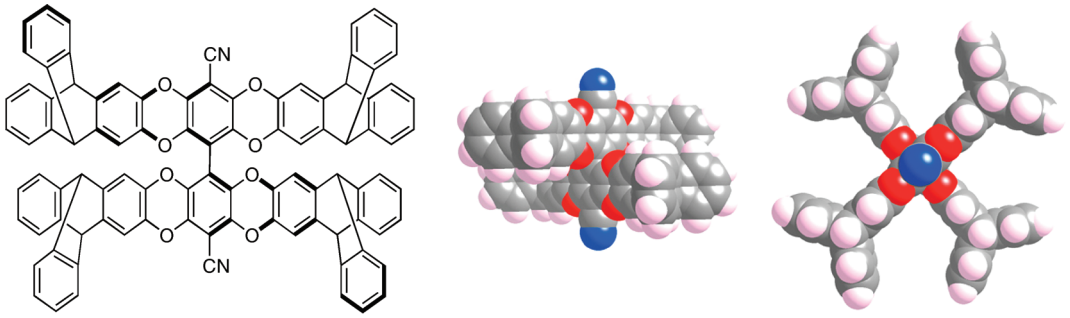

Figure 2. An example of an organic molecule of intrinsic microporosity (OMIM), which demonstrates significant microporosity in its amorphous solid state without possessing a macromolecular structure.[62]

The microporous non-network polymers, amorphous networks, and ordered organic networks assembled by the formation of rigid linking groups (via the reactions A−P depicted in Figure 3) between rigid monomers (**1**−**109**) are summarized in Tables 1−3, respectively. For non-network, soluble polymers it is relatively straightforward to attribute IM, as cross-linking is usually needed to stabilize a purely templated structure. Such non-network polymers are listed in Table 1. Structural units with well-defined cavities are provided by 1,1-spirobisindanes (e.g., **1**, **7**, **12**−**15**, **25**),[21,23−25,33,34] 9,9-spirobisfluorenes (e.g., **31**, **21**),[63] bisnaphthalenes (e.g., **5**, **23**),[33,64,65] 1,1-spirobis,2,3,4-tetrahydronaphthalenes (**16**−**19**),[22] and 9,10-ethanoanthracene (**8**, **9**).[24] For most of these polymers very significant microporosity is demonstrated by N_2 adsorption, with apparent BET surface areas in the range of 600−750 $m^2\ g^{-1}$. The soluble polymer that demonstrates the greatest IM (apparent BET surface area = 850 $m^2\ g^{-1}$) is derived from monomer **14**, which is based on the 1,1-spirobisindane framework to which has been fused two fluorene units via spiro-centers to provide additional concavities.[25] For PIMs, the fused ring linking group is formed using an efficient double aromatic nucleophilic substitution reaction between a catechol (1,2-dihydroaryl) and 1,2-difluoro- (or 1,2-dichloro-) aryl unit (Figure 3, reaction A).[33] More conventional polyimide synthesis (Figure 3, reaction B) can also be exploited by using the rigid bis(anhydride) spiro(bisindane) monomer **25**, with greater IM being obtained if the rotation about the imide C−N bonds is hindered by steric crowding, which is supplied by substituents on the diamine comonomer (e.g., **26**, **30**).[21,23,63,64] In contrast, the use of imide linking groups and concave-containing monomers within which there is relatively unhindered rotation (e.g., bisnaphthylene **23**) allows the lower limits of IM to be delineated for non-network polymers.[21,64] This demonstrates the strict requirement for the prevention of rotational freedom in order to provide IM in non-network polymers.

An assessment of the role of IM within amorphous network polymers is more problematic, and even the definition of IM as arising from the inefficient packing of "component macromolecules" is difficult to apply to networks, which are composed formally of a single macromolecule. At one extreme, hypercross-linked polystyrenes, although highly microporous, do not possess IM as the component polystyrene is relatively flexible and does not possess permanent concavities. Whereas, at the other extreme, network polymers derived from similar cavity-containing components such as 1,1-spirobisindane **1**,[35−37]

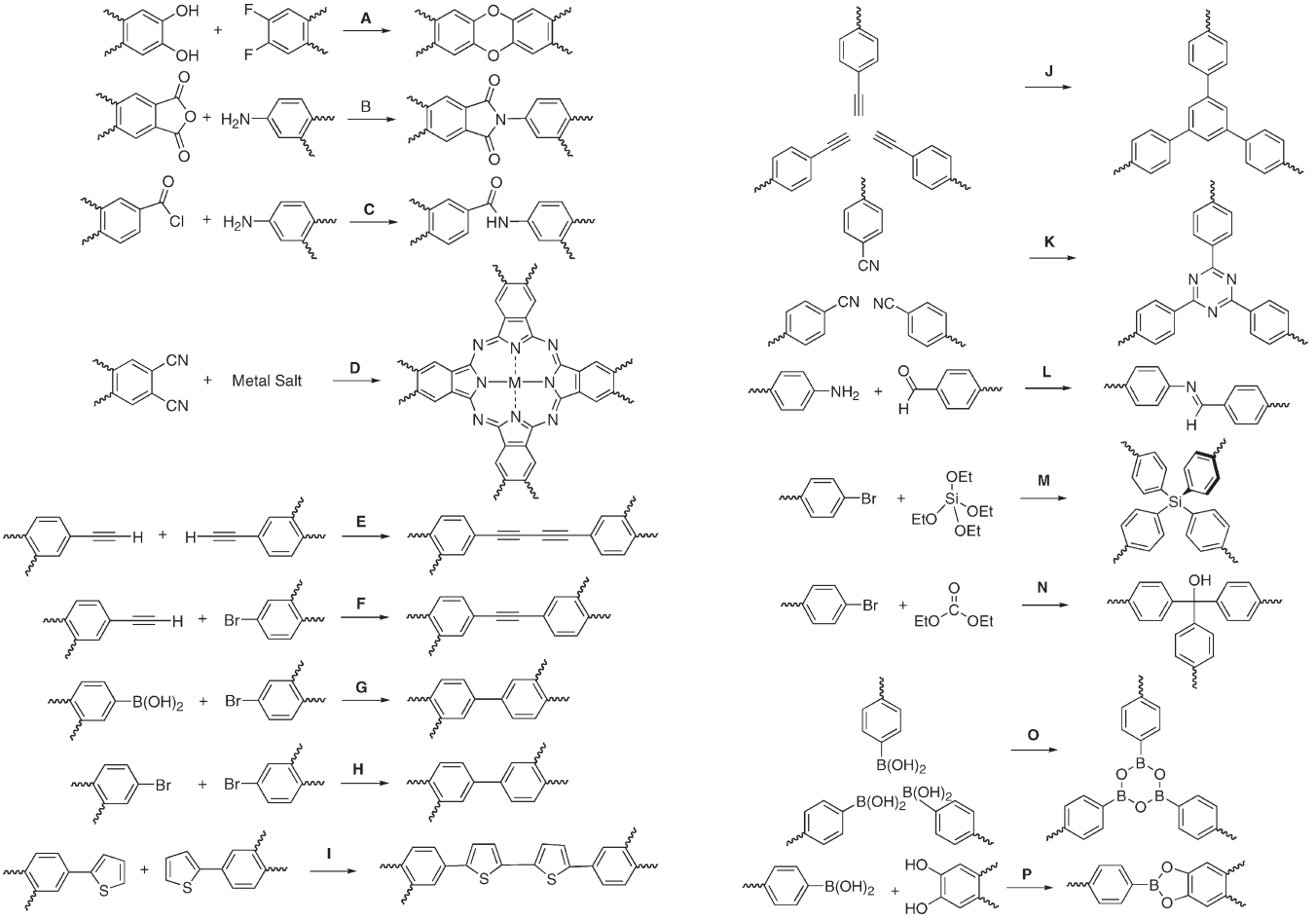

Figure 3. Reactions used to form rigid linkages between rigid monomers to prepare microporous polymers (Tables 1−3): (A) base-mediated aromatic nucleophilic substitution; (B) imide formation; (C) amide formation; (D) metal ion-mediated phthalocyanine formation; (E) Cu/Pd-mediated ethylynyl coupling; (F) Pd-mediated aryl−ethylynyl (Sonogashira−Hagihara) coupling; (G) Pd-mediated aryl−aryl (Suzuki) coupling; (H) $Ni(COD)_2$-mediated aryl−aryl (Yamamoto) coupling; (I) $FeCl_3$-mediated thiophenyl−thiophenyl oxidative coupling; (J) Co-mediated ethylynyl cyclotrimerization; (K) $ZnCl_2$ mediated nitrile cyclotrimerization; (L) imine formation; (M) lithium-mediated formation of tetraphenylsilane; (N) lithium-mediated formation of carbinols; (O) borate anhydride formation; (P) borate ester formation.

9,9-spirobisfluorenes (e.g., **42**),[66] or tetraphenylmethane (e.g., **43**)[67] as non-network PIMs, and that are connected by the same fused ring[27,35−37] or imide[66,67] linking groups, possess a subnanometer pore structure which must be ascribed to IM (Table 2). Although direct comparisons are difficult, it seems clear that networks possess greater microporosity than non-network polymers assembled from similar monomers, presumably due to macrocyclization. For example, the polyimide network derived from monomers **24** and **42** has an apparent BET surface area of 984 $m^2\ g^{-1}$, whereas that of the soluble polyimide from monomers **24** and **31** is only 554 $m^2\ g^{-1}$.[63,66] The most microporous amorphous network prepared to date using the concept of IM (apparent BET surface area = 1730 $m^2\ g^{-1}$) is that derived from triptycene monomer **36**.[26,68] The shape of this monomer constrains the growth of the polymer within the same plane to provide a rigid macromolecular structure with large concavities. The faces of the ribbonlike "struts" between the triptycenes are oriented perpendicular to the plane of the macromolecular growth. This arrangement blocks face-to-face association between these planar struts, leading to greater IM. For this network there is also likely to be a significant contribution to the IM from macrocycles.

For the attainment of microporosity in network polymers, it appears that the requirement for the prevention of rotation about single bonds is relaxed, presumably due to the network itself preventing structural rearrangement that could result in a collapse of the porous structure. Hence, the formation of rigid networks using metal-mediated ethynylene−ethynylene (Table 2; Figure 3, reaction E),[69] ethynylene−aryl (PAEs, reaction F),[70−74] or aryl−aryl (reactions G and H)[73,75] coupling reactions is compatible with obtaining highly microporous materials and provides what have been termed as conjugated microporous polymers (CMPs) by Cooper.[71,76] These materials demonstrate high apparent BET surface areas in the range 500−1300 $m^2\ g^{-1}$. An interesting structure−property relationship is evident for these materials in that the longer the linear struts between the branch points, the lower is the porosity.[70,77] This is opposite to what is found in MOFs and COFs (e.g., compare COF-6 and COF-8, Table 3) and is likely to relate to the longer struts having a larger number of bonds with rotational freedom, which will reduce IM. Other microporous networks have been prepared by reactions involving triazine formation from aromatic nitriles (Table 2; monomers **86**−**92**; Figure 3, reaction K),[77−81] alkyne trimerization (monomers **83** and **84**; reaction J), or phthalocyanine formation (monomer **41**; reaction D),[29,36] using concavity-containing monomers. An alternative strategy to similar materials, termed elemental organic frameworks (EOMs) by Rose,[82] involves the lithium-mediated synthesis of the concave molecular unit tetraphenylsilane (Figure 3, reaction M) during network formation from monomers **54** or **72** with **98**. This is a similar strategy to the preparation of hyper-cross-linked polycarbinol networks derived from monomers **71** and **99**−**102** via lithiation

Table 1. Non-Network Microporous Polymers Derived from Rigid Monomers (See Chart 1)

monomers	synthesis[a]	name[b]	surface area (BET; $m^2 g^{-1}$)	ref
1 + **2**	A	PIM-1	760	33, 34
1 + **3**	A	PIM-2	600	33
1 + **4**	A	PIM-3	560	33
5 + **2**	A	PIM-4	440	33
5 + **3**	A	PIM-5	540	33
6 + **3**	A	PIM-6	430	33
1 + **7**	A	PIM-7	680	24
8 + **7**	A	PIM-8	677	24
1 + **9**	A	PIM-9	661	24
8 + **9**	A	PIM-10	680	24
10 + **7**	A	Cardo-PIM-1	621	24
10 + **9**	A	Cardo-PIM-2	580	24
12 + **2**	A	polymer from 5	501	25
13 + **2**	A	polymer from 6	560	25
14 + **2**	A	polymer from 7	895	25
15 + **2**	A	polymer from 8	656	25
16 + **2**	A	polymer from 5	432	22
17 + **2**	A	polymer from 8	395	22
18 + **2**	A[c]	polymer from 10	713	22
19 + **2**	A	polymer from 14	203	22
20 + **2**	A	polymer from 15	590	22
21 + **2**	A	polymer from 16	300	22
1 + **22**	A	MP-1	679	117
23 + **24**	B	polyimide	57	64
25 + **26**	B	PIM-PI-1	680	21
25 + **26**	B	PIM-PI-2	500	21
25 + **27**	B	PIM-PI-3	471	21
25 + **28**	B	PIM-PI-4	486	21
25 + **29**	B	PIM-PI-7	485	21
25 + **30**	B	PIM-PI-8	683	21
24 + **31**	B	P4	551	63
31 + **32**	C	P3	156	63

[a] See Figure 3. [b] As given in reference. [c] It is thought that this molecule is cross-linked due to an additional Aldol reaction, which takes place during polymerization.

Table 2. Network Microporous Polymers Derived from Rigid Monomers (See Chart 2)

monomer(s)	synthesis[a]	name[b]	surface area (BET; $m^2 g^{-1}$)	ref
1 + **33**	A	Por-PIM	980	37
1 + **34**	A	HATN-PIM	775	35
2 + **35**	A	CTC-PIM	830	27
2 + **36**	A	Trip-PIM	1760	26, 68
37	A	MP-2	1050	117
1 + **39**	A	Pc-PIM	201	119
39	A	MP-2	1050	117
40	A	OFP-3	1159	116
41	D + metal salt	Pc-PIM	650−750	29, 36
42 + **24**	B	PI1	982	66
43 + **44**	B	polymer 5	750	67
45	E	HCMP-1	842	69
46	E	HCMP-2	827	69
45 + **47**	F	CMP-0	1018	70, 71
45 + **48**	F	CMP-1	834	70, 71
45 + **49**	F	CMP-2	634	70, 71
46 + **47**	F	CMP-3	522	70, 71
46 + **51**	F	CMP-4	744	70, 71
47 + **50**	F	CMP-5	512	70, 71
46 + **52**	F	P3	510	73
53 + **46**	F	E1	1213	72
53 + **45**	F	E2	448	72
54 + **46**	F	E3	1092	72
54 + **45**	F	E4	925	72
45 + **55**	F	NCMP-0	1108	74
55 + **56**	F	NCMP-1	968	74
55 + **47**	F	NCMP-2	900	74
55 + **48**	F	NCMP-3	866	74
55 + **49**	F	NCMP-4	546	74
45 + **57**	F	PAE from 1	136	90
45 + **58**	F	PAE from 2	867	90
45 + **59**	F	PAE from 3	682	90
45 + **60**	F	PAE from 4	247	90
45 + **61**	F	PAE from 5	739	90
45 + **62**	F	PAE from 6	723	90
45 + **63**	F	PAE from 7	690	90
45 + **64**	F	PAE from 8	761	90
45 + **65**	F	PAE from 9	648	90
45 + **66**	F	PAE from 10	293	90
45 + **67**	F	PAE from 11	140	90
45 + **68**	F	PAE from 12	322	90
45 + **69**	F	PAE from 13	853	90
45 + **70**	F	PAE from 14	803	90
45 + **71**	F	PAE from 15	3	90
45 + **72**	F	PAE from 16	204	90
45 + **73**	F	PAE from 17	42	90
45 + **74**	F	PAE from 18	262	90
45 + **75**	F	PAE from 19	880	90
45 + **76**	F	PAE from 20	542	90
45 + **77**	F	PAE from 21	637	90
45 + **78**	F	PAE from 22	779	90
52 + **79**	G	P1	450	73
52 + **80**	G	P2	210	73
52	H	YSN	1275	75
51	H	YBN	1255	75
51 + **52**	H		580	75
81	I	PS4TH	971	118
81	I	from 1	577	128
82	I	from 2	1060	128
83	J	PT4AC	762	118
84	J	PS4AC2	1043	118
42 + **85**	C	PA1	50	66
86	K	mDCB	850	79, 91
87	K	TCB	730	79
88	K	TCBP	1345	79
89	K	DCBP	1150	79
90	K	DCTP	1900	79
91	K	TCS	583	77
92	K	PAF-2	1109	80
93 + **94**	L	SNW-1	1377	19
93 + **95**	L	SNW-2	842	19
93 + **96**	L	SNW-3	1133	19
93 + **97**	L	SNW-4	1213	19
54 + **98**	M	EOF-1	780	82
72 + **98**	M	EOF-2	1046	82
72 + **99**	N		570	129
72 + **100**	N	polymer 1	1167	13, 129, 130
100 + **101**	N		561	13, 129, 130
100 + **102**	N		443	13, 129, 130

[a] See Figure 3. [b] As given in reference.

Table 3. Ordered Framework Polymers Derived from Rigid Monomers (See Chart 3)

monomer(s)	synthesis[a]	name[b]	surface area (BET; $m^2 g^{-1}$)	ref
79	O	COF-1	750	6, 131
79 + **103**	P	COF-5	1670	6, 131
103 + **104**	P	COF-6	750	131, 132
103 + **105**	P	COF-8	1350	131, 132
80 + **103**	P	COF-10	1760	131, 132
106	O	COF-102	3620	5, 131
107	O	COF-103	3530	5, 131
108	O	PPy-COF	923	133
43 + **94**	M	COF-300	1360	58
101	H	PAF-1	5600	92
109	L	CTF-1	791	79, 91

[a] See Figure 3. [b] As given in reference.

Chart 1

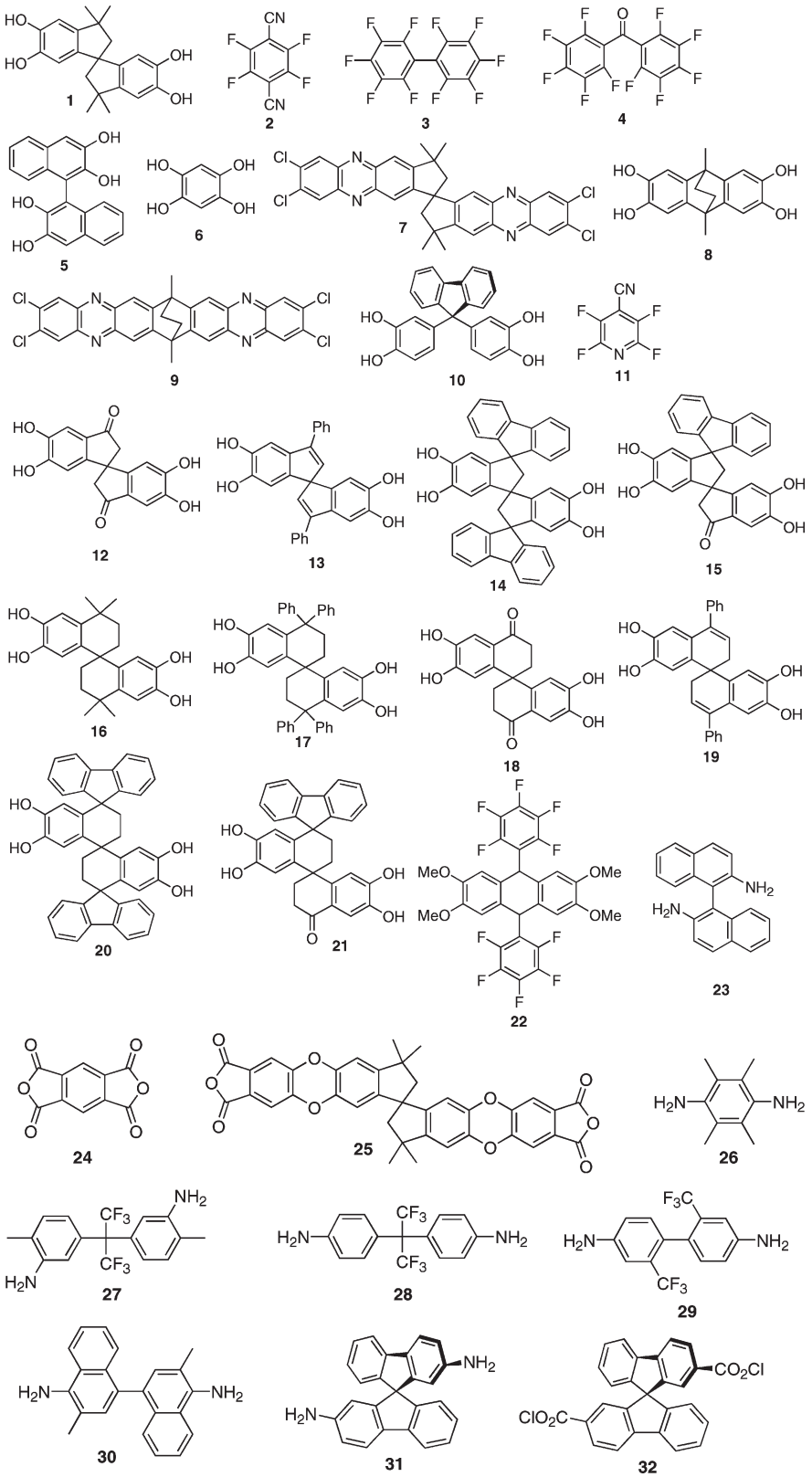

of aryl bromides (reaction N), described by Webster et al. in the early 1990s.[13,83,84] For EOMs the networks with longer struts between the silane nodes (i.e., biphenyl versus phenyl) demonstrated greater microporosity. Therefore, for amorphous microporous network polymers there appears to be a trade-off between the effect of enhancing the concavities by increasing the length of the internodal struts versus introducing bonds with unhindered rotation that can cause the collapse of the microporous structure.

Based on the concept of IM, a greater degree of rotational freedom and flexibility either within the concave molecular unit or in the linking group should reduce the contribution of IM to

Chart 2

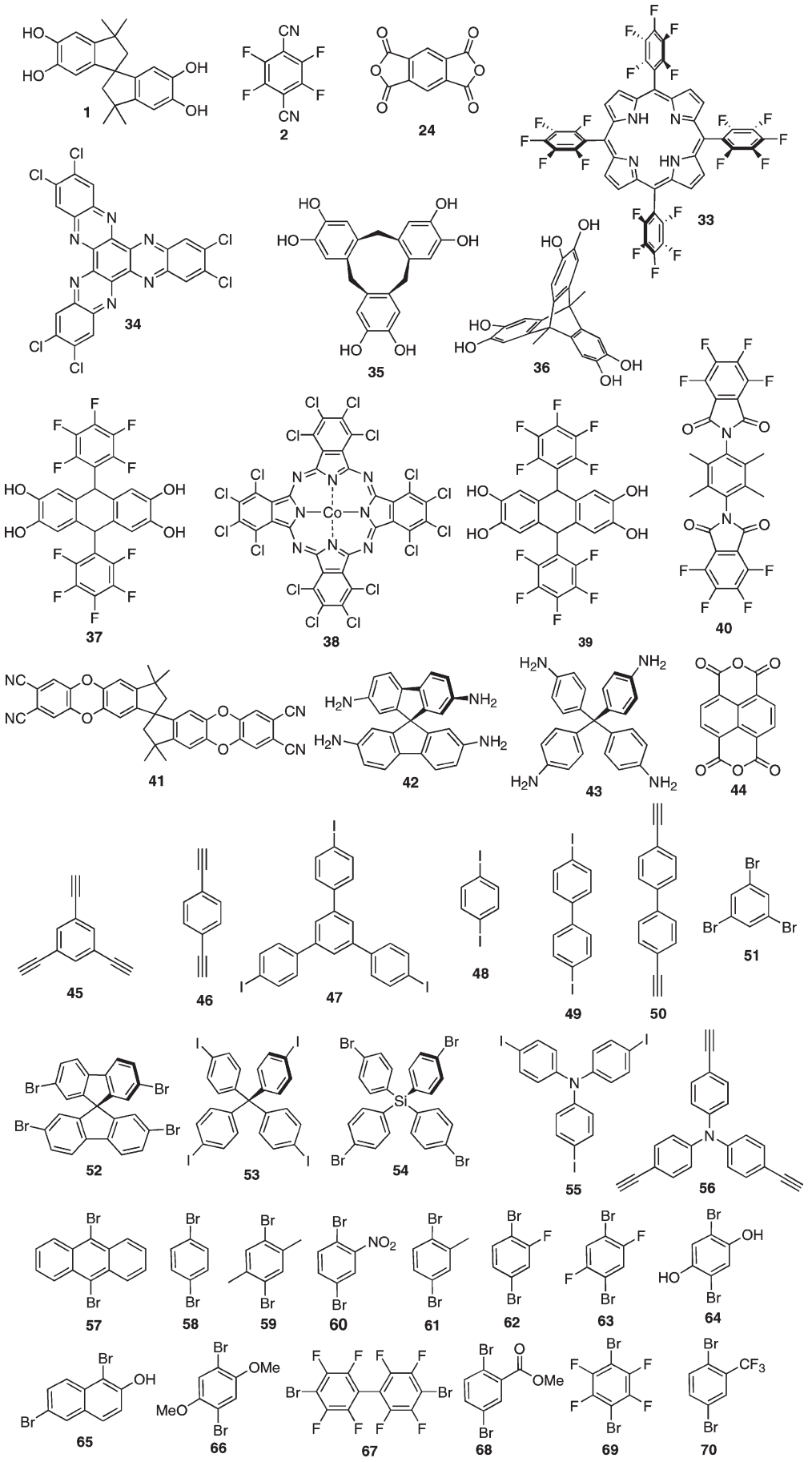
1
2
24
33
34
35
36
37
38
39
40
41
42
43
44
45
46
47
48
49
50
51
52
53
54
55
56
57
58
59
60
61
62
63
64
65
66
67
68
69
70

Chart 2 Continued

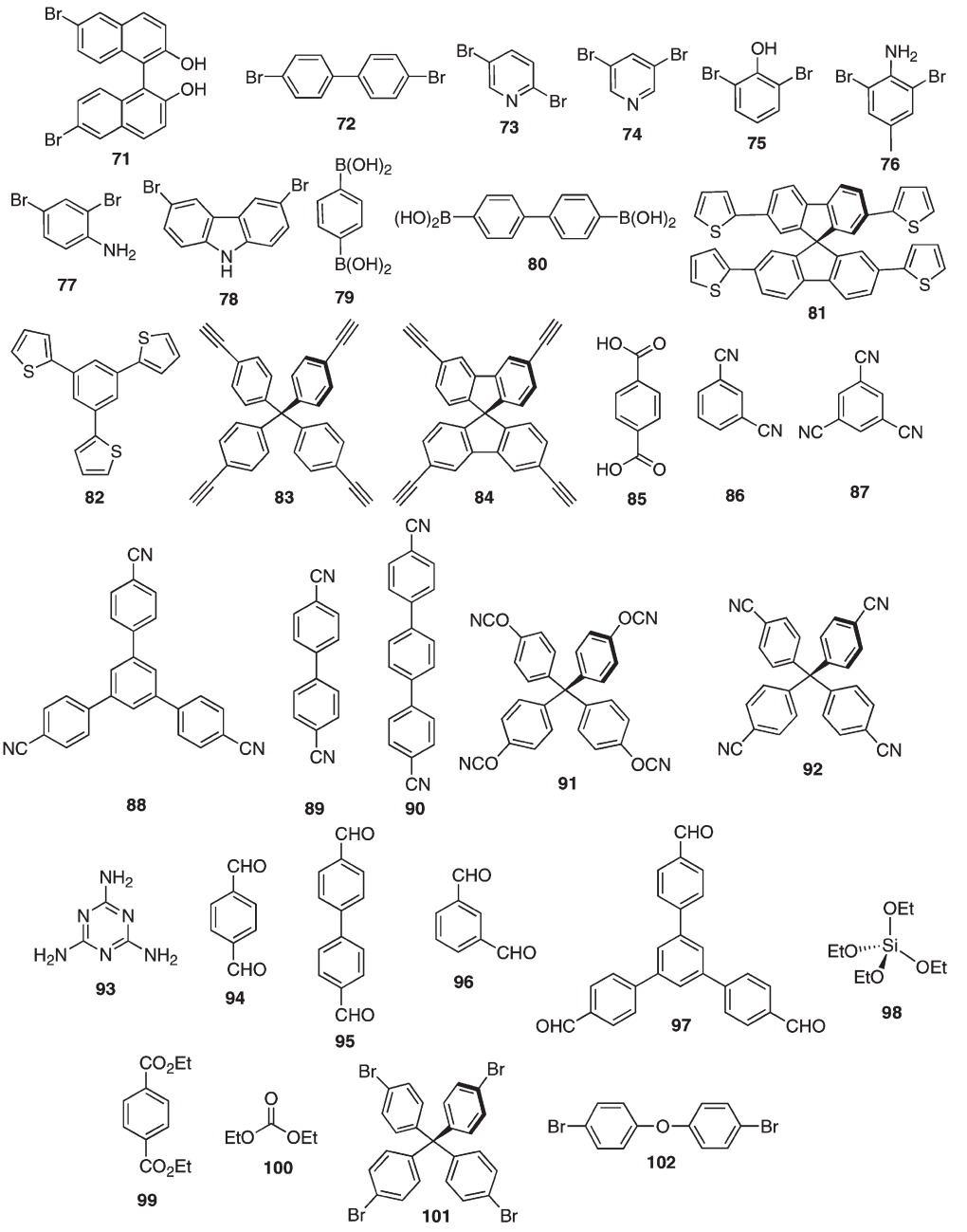

the porosity of the network.[66] However, can the loss of IM due to the extra flexibility of the network be compensated by an increase in microporosity arising from template effects? If so, is there a continuum for amorphous microporous networks, from those with IM to purely hyper-cross-linked polymers, as the flexibility of the network increases? Davankov et al., in their review of hyper-cross-linked polymers,[9] predicted that many types of polymer could be made microporous by the introduction of extensive cross-linking, so long as the correct solvent is employed as template. Their optimism has proved correct.[9,10,13−19] However, it is clear that most network polymers do not demonstrate significant microporosity by N_2 adsorption. For example, those which incorporate long alkyl chains within the framework are not microporous,[13] presumably due to their flexibility allowing the collapse of porosity during solvent removal. Long alkyl chains laterally attached to a rigid COF[85] or PIM[68] framework also reduce microporosity by a pore-blocking effect. Networks composed of rigid concave units linked by amide bonds[66] are found to be nonporous, which may be due to strong internetwork hydrogen bonding combining with a degree of rotational freedom to prevent the development of IM. However, it is possible that such amide-linked networks could be microporous if formed in the presence of a suitable template, as is the case for molecularly imprinted polymers, which are usually derived from hydrogen-bonding polymers and can possess significant microporosity (BET surface areas > 300 m^2 g^{-1}).[86−89] It is notable that several PAEs with large microporosity can be prepared, which incorporate −OH or $-NH_2$ groups (e.g., from monomers **64**, **65**, **76**, or **77**) that can act as strong H-bonding donors. These network are prepared in the presence of triethylamine, which may be acting as a H-bond accepting template.[90] In contrast, networks with true IM should demonstrate microporosity that is independent of the presence of a template during formation. Without studies to demonstrate the absence of *extrinsic* microporosity for a particular polymer system, it seems sensible to classify those amorphous microporous networks that contain single bonds with

Chart 3

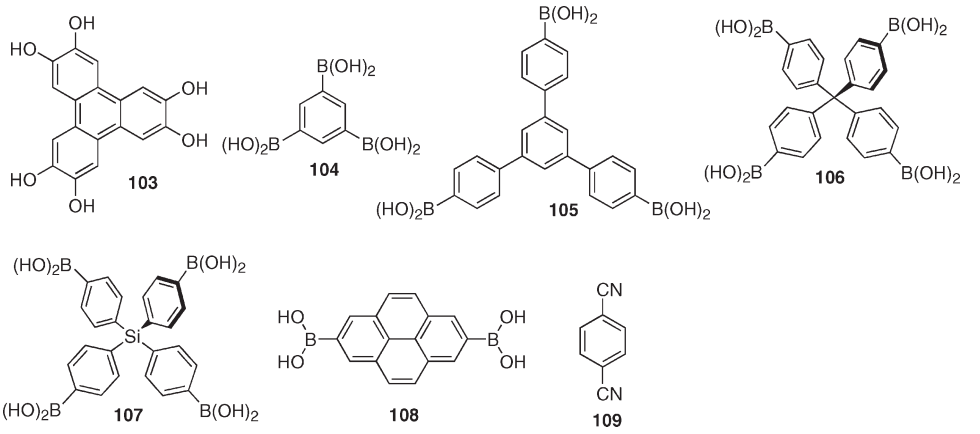

unhindered rotation (e.g., biphenyl, ethylyene, etc.) as hypercross-linked polymers.

Crystalline polymers such as COFs represent the optimal porous structure obtainable for a given concave molecular unit. COFs are prepared by linking the apexes of the unit (e.g., triphenylene **103**, tetraphenylmethane **106**, etc.) using borate anhydride[5,6] borate ester,[5,6] or enamine[58] formation to provide the open frameworks (Table 3; Figure 3, reactions O, P, and M, respectively). Other synthetic methods such as triazine formation (reaction K) and Yamamoto aryl−aryl coupling (reaction H) also appear to provide crystalline porous polymer networks termed a covalent triazine-based framework (CTF-1)[79,91] and a porous aromatic framework (PAF-1), respectively, with the latter apparently demonstrating the highest surface area of any porous material (BET surface area $> 7000\ m^2\ g^{-1}$).[92] In each case, strong but rapidly reversible covalent bonds dictate the low-density packing, with additional thermodynamic stability being provided by the inclusion of solvent (or molten metal salts in the case of the CTFs) within the pores during the assembly of the organic framework.

Characterization of Pore Structure

In order to understand how molecular structure influences the pore structure and hence the properties of a microporous polymer-based material, methods are needed for characterizing the pore structure in terms of, e.g., pore size distribution. A variety of experimental methods may be employed to investigate microporosity in amorphous materials. For example, small-angle X-ray scattering has been applied to microporous carbons[93] and ^{129}Xe NMR has been applied to glassy polymers.[94,95] Here, we focus on gas sorption analysis, positron annihilation lifetime spectroscopy, and computational techniques.

Gas Sorption Analysis. Microporous and mesoporous materials are commonly characterized by N_2 adsorption/desorption at liquid nitrogen temperature (77 K). At the lowest pressures, the very smallest pores accessible to N_2 are filled because multiwall interactions give rise to enhanced adsorption. On increasing the pressure, progressively larger pores are filled. Above a certain size (in practice around 2 nm), the mechanism of pore filling changes, with condensate building from the walls toward the center. This represents the transition from micropores to mesopores. Mesopores are often associated with a hysteresis loop; the desorption curve lies above the adsorption curve because desorption has to occur by evaporation from a liquid meniscus. The hysteresis loop associated with mesoporosity always closes at a relative pressure $p/p^\circ \geq 0.4$, where p° is the saturation pressure. There are various methodologies for calculating pore size distributions in the micropore and mesopore regions.

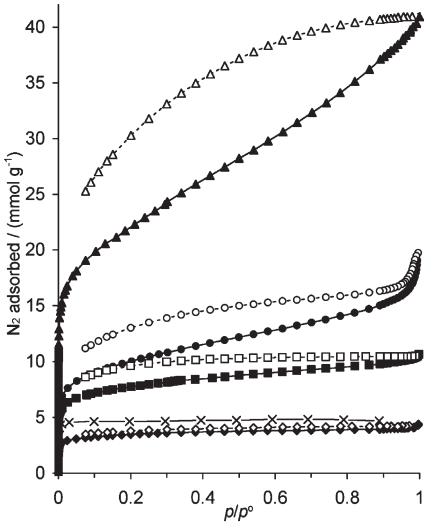

Figure 4. Experimental N_2 adsorption (filled symbols) and desorption (open symbols) isotherms at 77 K for a microporous crystal formed by 3,3′,4,4′-tetra(trimethylsilylethynyl)biphenyl[55] (◆, ◇), a network-PIM incorporating cobalt phthalocyanine[29] (■, □), the soluble, membrane-forming polymer PIM-1[107] (●, ○), a network-PIM based on methyltriptycene[68] (▲, △), and an isotherm calculated from a static atomistic packing model of PIM-1 (×).[100]

Given its history for characterizing other types of microporous material, high N_2 uptake at low p/p° may be taken as the primary indicator of microporosity in polymer-based materials. Figure 4 compares typical N_2 adsorption/desorption isotherms for a microporous crystal formed by 3,3′,4,4′-tetra(trimethylsilylethynyl)biphenyl,[55] a network-PIM incorporating cobalt phthalocyanine (from monomer **41**; reaction D),[29,36] the soluble, membrane-forming polymer PIM-1 (from monomers **1** and **2**; reaction A),[33,34] and a network-PIM based on methyltriptycene (monomers **2** and **36**; reaction A).[26,68] All these materials exhibit the low-pressure uptake characteristic of microporosity. The crystal shows minimal hysteresis, but the polymer-based materials all exhibit increasing uptake with increasing relative pressure and a hysteresis that extends down to low relative pressures. However, the hysteresis does not form a closed loop, as observed for mesoporous materials. Instead, it has to be attributed to plasticization and swelling of the polymer or to the tortuosity of the micropore structure.

The distribution of micropore size can be calculated from the very low pressure region of a N_2 adsorption isotherm by the Horvath−Kawazoe (HK) method.[96] In this method it is

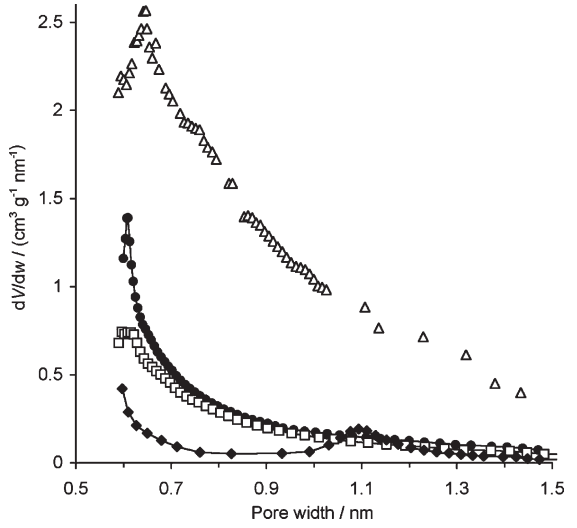

Figure 5. Pore size distributions determined from N_2 adsorption at 77 K by the HK method for a microporous crystal formed by 3,3′,4,4′-tetra-(trimethylsilylethynyl)biphenyl[55] (◆), a network-PIM incorporating cobalt phthalocyanine[29] (□), the soluble, membrane-forming polymer PIM-1[107] (●), and a network-PIM based on methyltriptycene[68] (△).

assumed that all pores of a certain size will fill at a particular relative pressure. It was originally derived for slit-shaped pores in a carbonaceous material but has subsequently been adapted to other pore geometries and types of material. Figure 5 shows micropore distributions calculated by the HK method from the experimental isotherms of Figure 4. For the crystal, the structure is known from X-ray single crystal analysis. It contains a bicontinuous network of open channels of 0.4 nm minimum diameter, connecting voids of 1.1 nm maximum diameter. The larger voids at 1.1 nm are clearly seen in the HK pore size distribution. The smaller channels would fill at a pressure lower than is experimentally achievable, so the uptake associated with them appears at a larger apparent size, around 0.6 nm. The broad agreement between the crystal structure and the HK distribution gives some confidence in the use of N_2 adsorption for micropore analysis, although the distortion of the distribution at the experimental limit needs to be kept in mind. For the three polymer samples in Figure 5 we see evidence of a broad distribution of pore size in the micropore (< 2 nm) region.

Molecular probes other than N_2 can be utilized in a similar way. In particular, CO_2 can be used to extend the distribution to smaller micropore size. This is demonstrated for PIM-1 in Figure 6, which compares pore size distributions from HK analysis of CO_2 adsorption at 303 K with that from N_2 adsorption. Figure 6 also includes results from positron annihilation lifetime spectroscopy (PALS) and computer modeling, which are discussed further below.

Positron Annihilation Lifetime Spectroscopy (PALS). Orthopositronium (o-Ps), a metastable particle produced by the reaction of a positron with an electron, is the ultimate probe of the empty spaces in a material. In a vacuum, o-Ps has an average lifetime of 142 ns, but within matter this is reduced because the o-Ps can "pick off" electrons and annihilate. In a polymer, o-Ps tends to be localized in free volume elements or holes, in which case its lifetime decreases with decreasing hole size. If assumptions are made about the shape of the hole (e.g., spherical or cylindrical), the hole size can be calculated using the Tao−Eldrup model.[97,98] In high free volume polymers, such as PIM-1, more than one o-Ps lifetime may be measured, which can be interpreted in terms of either a broad or a bimodal distribution of hole size.

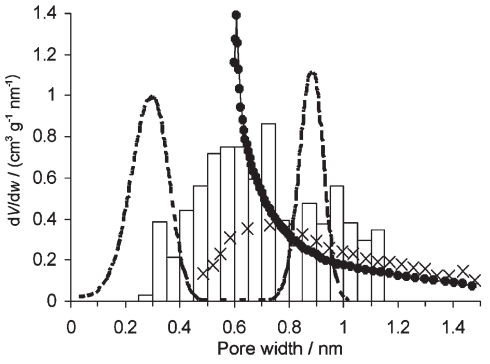

Figure 6. Comparison of pore size distributions for PIM-1 determined from N_2 adsorption at 77 K (●), CO_2 adsorption at 303 K (×) [data courtesy of Gregory Larson, Pennsylvania State University, and Nhamo Chaukura, University of Manchester], positron annihilation lifetime spectroscopy (---),[99] and calculated by computer simulation (grand canonical Monte Carlo method) (bars).[100]

Figure 6 shows a hole size distribution obtained for PIM-1 from PALS, assuming a bimodal distribution.[99] PALS confirms that the polymer contains free volume elements or voids in the size range associated with microporosity. However, as with other experimental techniques, the shape of the distribution depends on the model used.

Atomistic Computer Simulation. While there is ambiguity in the micropore distributions obtained from experimental data, further insight can be achieved through computer modeling. Figure 6 includes a pore size distribution, appropriate for a probe the size of a nitrogen molecule, determined for three packing models of PIM-1.[100] The data in Figure 6, which were obtained by a method that divides complex regions of free volume into smaller elements, are consistent with a broad distribution of pore size in the micropore range. The model is for a static system, without any consideration of polymer dynamics. It may be considered to represent the "instantaneous" porosity, excluding effects of plasticization, structural relaxation, or swelling due to the presence of the probe. The N_2 adsorption isotherm calculated for this static system is included in Figure 4. It shows a plateau (corresponding to micropore filling) with an effective surface area of 435 $m^2\ g^{-1}$. The additional uptake and hysteresis observed in the experimental isotherm for PIM-1 in Figure 4 may be attributed to the effects of polymer dynamics and the influence of the probe.

A variety of experimental techniques, and atomistic computer simulation, all support the contention that PIMs and related polymer-based materials are microporous as defined by IUPAC (pore size < 2 nm). However, there is as yet no unequivocal means of describing and characterizing the detailed pore structure or of accounting fully for the effects of polymer dynamics. Experimentally, improved methodologies are needed for characterizing microporous materials in terms of pore size distribution. Computationally, there is a need to link static behavior to dynamic effects in order to establish and predict the interrelationships between the molecular structure of a polymer, the effective pore structure, and the useful properties of the material.

Applications of Microporous Polymer-Based Materials

The drive to explore the concept of intrinsic microporosity, and so to develop new types of polymer-based microporous material, arises from the advantages of combining microporosity with the processability of a polymer. In particular, the ability to generate soluble, and hence solution-processable, film-forming microporous materials offers unique benefits.

Many key technological challenges involve molecular separations, whether on a massive scale, such as the capture of greenhouse gases, or on a tiny scale, as in the detection of trace contaminants. Intrinsically microporous materials can selectively take up and transport molecular species, making them useful in membranes and as adsorbents. Further applications arise from the incorporation of catalytic functionality and by utilizing the optical and electronic properties of the materials. Some promising avenues of exploitation are outlined below.

Membranes. Membrane technology provides a route to energy-efficient, cost-effective processes for a wide range of industries. Of particular interest are processes for the separation of liquid, gas, and vapor mixtures. In all membrane separations, there is a balance between the separation that is achievable (expressed in terms of a separation factor or selectivity) and the productivity (expressed as a flux or permeance). In general, it is desirable to maximize the productivity, so as to minimize the membrane area required, and the challenge is to develop membrane materials that show improved separation with high flux.

Pervaporation Membranes. In pervaporation, the feed is a liquid mixture and the permeate is removed as a vapor. The driving force for transport comes from application of a vacuum or sweep gas to the permeate side of the membrane. An advantage of pervaporation is that it can be used to break an azeotrope. Commercial pervaporation plants, e.g., for dehydration of ethanol/water mixtures, commonly employ hydrophilic membranes. However, there is increasing interest in hydrophobic membranes for wastewater treatment and for the separation of organic−organic mixtures. Pervaporation was the first application of PIM membranes to be investigated. PIM-1 was shown to form a hydrophobic membrane, selectively transporting organics, such as phenol and aliphatic alcohols, from mixtures with water. High flux, coupled with good separation factor and stability, makes this a promising area for further development.[34,101]

Nanofiltration Membranes. In nanofiltration, a pressure is applied to a liquid feed. Unlike pervaporation, there is no phase change on permeation. The membrane retains molecules above a certain size. This is a well-established technology for treating aqueous feeds. An area with significant potential for growth is that of solvent-resistant nanofiltration for the treatment of organic mixtures.[102] Membranes of PIM-1 and PIM copolymers show promise in this respect.[101,103]

Gas Separation Membranes. In membrane gas separation, the driving force comes from a pressure difference across the membrane.[41] For a given gas pair, the trade-off between permeability (permeance multiplied by membrane thickness) and selectivity (expressed as a ratio of permeabilities) may be represented by a double-logarithmic plot of selectivity against the permeability of the fastest species (Figure 7). In 1991, Robeson plotted data in this way for a wide range of polymers, demonstrating an empirical upper bound.[104] When PIMs were developed, they were shown to cross the 1991 upper bound for important gas pairs such as O_2/N_2 and CO_2/CH_4.[105] This contributed to Robeson's revision of the upper bound in 2008.[106] In common with other glassy polymers, the transport properties of PIMs are dependent on their processing history. In particular, a methanol treatment, which helps flush out residual solvent and allows relaxation of the polymer chains, can significantly enhance permeability (see Figure 7).[107] The transport properties of PIM membranes can be tailored through chemical modification such as carboxylation[108] and through the incorporation of comonomers.[65,109,110] A further approach to improving membrane performance is the formation of mixed-matrix membranes.[111]

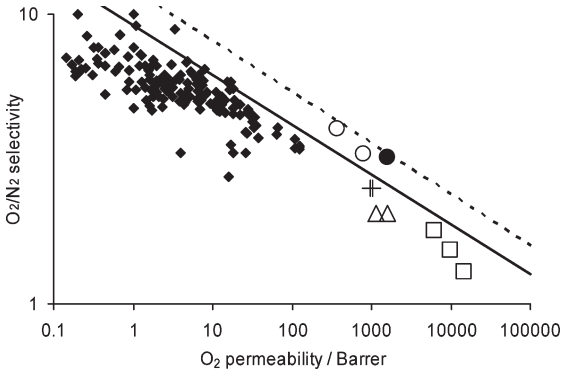

Figure 7. Double-logarithmic plot of O_2/N_2 selectivity versus O_2 permeability showing Robeson's 1991 (solid line)[104] and 2008 (dashed line)[106] upper bounds and experimental data for PIM-1 (○),[99,105] PIM-1 after methanol treatment (●),[107] addition-type poly(trimethylsilylnorbornene)(+),[123,124] Teflon AF2400 (△)[125,126] poly(trimethylsilylpropyne) (□),[127] and various other polymers which have been studied since 1991 (◆). Units of permeability: 1 barrer = 10^{-10} cm^3 [STP] cm cm^{-2} s^{-1} cmHg^{-1} = 3.35×10^{-16} mol m m^{-2} s^{-1} Pa^{-1}.

Adsorbents for Water Treatment. There is a long history of the use of microporous materials as solid-state adsorbents. Polymer-based microporous materials offer the potential for fine-tuning the functionality and pore structure for specific adsorption processes. Being organic, they have a particular affinity for organic species. Thus, network-PIMs show selective uptake of phenol[35] and small dye molecules[29] from aqueous solution.

Adsorbents for Gas Storage. Porous polymers of various types have been investigated for methane storage[14] and hydrogen storage.[15,18,26,27,112−118] The latter is of particular significance for vehicles powered by hydrogen−oxygen fuel cells. For a weakly adsorbing gas such as H_2, adsorption is enhanced in very small pores (ultramicropores, width ca. 0.7 nm) because of multiwall interactions. As indicated above, PIMs have a relatively high concentration of pores in this size range. The challenge is to increase the capacity while retaining a favorable pore structure.

Catalysis. The PIM concept originally developed from work aimed at incorporating metallophthalocyanines[36] and metalloporphyrins[37] into networks that allowed access to their catalytic metal centers. It has been demonstrated that phthalocyanine and porphyrin network-PIMs are more effective as heterogeneous catalysts than their low molar mass analogues, in test reactions such as the oxidation of hydroquinone.[119] A cobalt phthalocyanine network-PIM has been shown to be effective for the catalytic desulfurization of salt water.[120] A hexazatrinaphthylene-based network-PIM[35] binds palladium, giving an effective catalyst for Suzuki carbon−carbon coupling reactions. Similarly, palladium nanoparticles have been incorporated within a conjugated PAE network by processing in supercritical CO_2.[121] Therefore, we anticipate that intrinsically microporous polymer-based materials will play an increasing role in the application of flow chemistry on the laboratory and industrial scale.

Sensors. A recently reported optical sensor exploits the rapid change in refractive index of a thin film of PIM-1 on adsorption of organic vapor to provide a dramatic green-to-red color change, which can be visualized for sensing concentrations down to 5 ppm or detected by a fiber-optic spectrometer down to 50 ppb.[122] The response is general for all organic vapors, but the hydrophobic nature of PIM-1 ensures the lack of interference by humidity. The fabrication and performance of this device both benefit from the unique

combination of solvent processability and microporosity of the PIM component.

Conclusions

Materials with cavities or channels of molecular dimensions (i.e., microporous materials as defined by IUPAC, having pore sizes <2 nm) find widespread application in separations and catalysis. The desire to combine the properties of a microporous material with the processability of a polymer has prompted significant research in recent years. *Extrinsic* microporosity in hyper-cross-linked and molecularly imprinted polymers arises from the template effects of solvent or other small molecules. *Intrinsic* microporosity forms as a direct consequence of the shape and rigidity of the macromolecular chain. An essential feature of a material with intrinsic microporosity is the presence of rigid structural components with well-defined concavities. To create a polymer of intrinsic microporosity (PIM), such components must be linked in a way that prevents collapse of the micropore structure. This requires linking groups with no significant rotational freedom about backbone bonds.

In order to establish the relationships between macromolecular structure, pore structure, and properties, reliable methods are needed for characterizing the pore size distribution. Gas adsorption (N_2 at 77 K; CO_2 at 303 K), positron annihilation lifetime spectroscopy, and computer simulation all provide insight into micropore structure, but further research is needed to refine the methodologies used and fully to understand the influence of polymer dynamics on the behavior of microporous polymer-based materials.

Acknowledgment. We thank the past and present members of our research groups for their contribution to the development of PIMs and EPSRC for funding.

References and Notes

(1) *Handbook of Porous Solids*; Schüth, F., Sing, K., Weitkamp, J., Eds.; Wiley-VCH: Berlin, 2002; Vols. *1*−*5*.
(2) Eddaoudi, M.; Kim, J.; Rosi, N.; Vodak, D.; Wachter, J.; O'Keefe, M.; Yaghi, O. M. *Science* **2002**, *295*, 469–472.
(3) Eddaoudi, M.; Moler, D. B.; Li, H.; Chen, B.; Reinke, T. M.; O'Keefe, M.; Yaghi, O. M. *Acc. Chem. Res.* **2001**, *34*, 316–330.
(4) Ferey, G. *Chem. Soc. Rev.* **2008**, *37*, 191–214.
(5) El-Kaderi, H. M.; Hunt, J. R.; Mendoza-Cortes, J. L.; Cote, A. P.; Taylor, R. E.; O'Keeffe, M.; Yaghi, O. M. *Science* **2007**, *316*, 268–272.
(6) Cote, A. P.; Benin, A. I.; Ockwig, N. W.; O'Keeffe, M.; Matzger, A. J.; Yaghi, O. M. *Science* **2005**, *310*, 1166–1170.
(7) Hoskins, B. F.; Robson, R. *J. Am. Chem. Soc.* **1989**, *111*, 5962–5964.
(8) Brunauer, S.; Emmett, P. H.; Teller, E. *J. Am. Chem. Soc.* **1938**, *60*, 309–319.
(9) Tsyurupa, M. P.; Davankov, V. A. *React. Funct. Polym.* **2002**, *53*, 193–203.
(10) Davankov, V. A.; Rogozhin, S. V.; Tsyurupa, M. P. US Patent 3,729,457, 1971.
(11) Tsyurupa, M. P.; Davankov, V. A. *React. Funct. Polym.* **2006**, *66*, 768–779.
(12) Ahn, J. H.; Jang, J. E.; Oh, C. G.; Ihm, S. K.; Cortez, J.; Sherrington, D. C. *Macromolecules* **2006**, *39*, 627–632.
(13) Urban, C.; McCord, E. F.; Webster, O. W.; Abrams, L.; Long, H. W.; Gaede, H.; Tang, P.; Pines, A. *Chem. Mater.* **1995**, *7*, 1325–13332.
(14) Wood, C. D.; Tan, B.; Trewin, A.; Su, F.; Rosseinsky, M. J.; Bradshaw, D.; Sun, Y.; Zhou, L.; Cooper, A. I. *Adv. Mater.* **2008**, *20*, 1916–1920.
(15) Germain, J.; Frechet, J. M. J.; Svec, F. *J. Mater. Chem.* **2007**, *17*, 4989–4997.
(16) Germain, J.; Frechet, J. M. J.; Svec, F. *Chem. Commun.* **2009**, 1526–1528.
(17) Germain, J.; Svec, F.; Frechet, J. M. J. *Chem. Mater.* **2008**, *20*, 7069–7076.
(18) Svec, F.; Germain, J.; Frechet, J. M. J. *Small* **2009**, *5*, 1098–1111.
(19) Schwab, M. G.; Fassbender, B.; Spiess, H. W.; Thomas, A.; Feng, X. L.; Mullen, K. *J. Am. Chem. Soc.* **2009**, *131*, 7216–7217.
(20) Haupt, K.; Mosbach, K. *Chem. Rev.* **2000**, *100*, 2495–2504.
(21) Ghanem, B. S.; McKeown, N. B.; Budd, P. M.; Al-Harbi, N. M.; Fritsch, D.; Heinrich, K.; Starannikova, L.; Tokarev, A.; Yampolskii, Y. *Macromolecules* **2009**, *42*, 7881–7888.
(22) Carta, M.; Msayib, K. J.; McKeown, N. B. *Tetrahedron Lett.* **2009**, *50*, 5954–5957.
(23) Ghanem, B. S.; McKeown, N. B.; Budd, P. M.; Fritsch, D. *Adv. Mater.* **2008**, *20*, 2766–2771.
(24) Ghanem, B. S.; McKeown, N. B.; Budd, P. M.; Fritsch, D. *Macromolecules* **2008**, *41*, 1640–1646.
(25) Carta, M.; Msayib, K. J.; Budd, P. M.; McKeown, N. B. *Org. Lett.* **2008**, *10*, 2641–2643.
(26) Ghanem, B.; McKeown, N. B.; Harris, K. D. M.; Pan, Z.; Budd, P. M.; Butler, A.; Selbie, J.; Book, D.; Walton, A. *Chem. Commun.* **2007**, 67–69.
(27) McKeown, N. B.; Gahnem, B.; Msayib, K. J.; Budd, P. M.; Tattershall, C. E.; Mahmood, K.; Tan, S.; Book, D.; Langmi, H. W.; Walton, A. *Angew. Chem., Int. Ed.* **2006**, *45*, 1804–1807.
(28) McKeown, N. B.; Budd, P. M. *Chem. Soc. Rev.* **2006**, *35*, 675–683.
(29) Maffei, A. V.; Budd, P. M.; McKeown, N. B. *Langmuir* **2006**, *22*, 4225–4229.
(30) McKeown, N. B.; Budd, P. M.; Msayib, K. J.; Ghanem, B. S.; Kingston, H. J.; Tattershall, C. E.; Makhseed, S.; Reynolds, K. J.; Fritsch, D. *Chem.—Eur. J.* **2005**, *11*, 2610–2620.
(31) Makhseed, S.; McKeown, N. B.; Msayib, K.; Bumajdad, A. *J. Mater. Chem.* **2005**, *15*, 1865–1870.
(32) Budd, P. M.; McKeown, N. B.; Fritsch, D. *J. Mater. Chem.* **2005**, *15*, 1977–1986.
(33) Budd, P. M.; Ghanem, B. S.; Makhseed, S.; McKeown, N. B.; Msayib, K. J.; Tattershall, C. E. *Chem. Commun.* **2004**, 230–231.
(34) Budd, P. M.; Elabas, E. S.; Ghanem, B. S.; Makhseed, S.; McKeown, N. B.; Msayib, K. J.; Tattershall, C. E.; Wang, D. *Adv. Mater.* **2004**, *16*, 456–460.
(35) Budd, P. M.; Ghanem, B.; Msayib, K.; McKeown, N. B.; Tattershall, C. *J. Mater. Chem.* **2003**, *13*, 2721–2726.
(36) McKeown, N. B.; Makhseed, S.; Budd, P. M. *Chem. Commun.* **2002**, 2780–2781.
(37) McKeown, N. B.; Hanif, S.; Msayib, K.; Tattershall, C. E.; Budd, P. M. *Chem. Commun.* **2002**, 2782–2783.
(38) McKeown, N. B.; Budd, P. M. In *Encyclopedia of Polymer Science and Technology*; Wiley: New York, 2009; DOI: 10.1002/0471440264.pst563.
(39) Ilinitch, O. M.; Fenelonov, V. B.; Lapkin, A. A.; Okkel, L. G.; Terskikh, V. V.; Zamaraev, K. I. *Microporous Mesoporous Mater.* **1999**, *31*, 97–110.
(40) Dunitz, J. D.; Filippini, G.; Gavezzotti, A. *Helv. Chim. Acta* **2000**, *83*, 2317–2335.
(41) Budd, P. M.; McKeown, N. B. *Polym. Chem.* **2010**, *1*, 63–68.
(42) Aste, T.; Weare, D. *The Pursuit of Perfect Packing*; Chapman and Hall: London, 2008.
(43) Torquato, S.; Jiao, Y. *Phys. Rev. E* **2009**, 80.
(44) Dunitz, J. D.; Filippini, G.; Gavezzotti, A. *Tetrahedron* **2000**, *56*, 6595–6601.
(45) Jiao, Y.; Stillinger, F. H.; Torquato, S. *Phys. Rev. E* **2009**, 79.
(46) Jiao, Y.; Stillinger, F. H.; Torquato, S. *Phys. Rev. Lett.* **2008**, *100*, 4.
(47) Long, T. M.; Swager, T. M. *Adv. Mater.* **2001**, *13*, 601–604.
(48) Tsui, N. T.; Yang, Y.; Mulliken, A. D.; Torun, L.; Boyce, M. C.; Swager, T. M.; Thomas, E. L. *Polymer* **2008**, *49*, 4703–4712.
(49) Swager, T. M. *Acc. Chem. Res.* **2008**, *41*, 1181–1189.
(50) Tsui, N. T.; Torun, L.; Pate, B. D.; Paraskos, A. J.; Swager, T. M.; Thomas, E. L. *Adv. Funct. Mater.* **2007**, *17*, 1595–1602.
(51) Tsui, N. T.; Paraskos, A. J.; Torun, L.; Swager, T. M.; Thomas, E. L. *Macromolecules* **2006**, *39*, 3350–3358.
(52) Thomas, S. W.; Long, T. M.; Pate, B. D.; Kline, S. R.; Thomas, E. L.; Swager, T. M. *J. Am. Chem. Soc.* **2005**, *127*, 17976–17977.
(53) Amara, J. P.; Swager, T. M. *Macromolecules* **2004**, *37*, 3068–3070.
(54) Long, T. M.; Swager, T. M. *J. Mater. Chem.* **2002**, *12*, 3407–3412.
(55) Msayib, K. J.; Book, D.; Budd, P. M.; Chaukura, N.; Harris, K. D. M.; Helliwell, M.; Tedds, S.; Walton, A.; Warren, J. E.; Xu, M. C.; McKeown, N. B. *Angew. Chem., Int. Ed.* **2009**, *48*, 3273–3277.
(56) Tozawa, T.; Jones, J. T. A.; Swamy, S. I.; Jiang, S.; Adams, D. J.; Shakespeare, S.; Clowes, R.; Bradshaw, D.; Hasell, T.; Chong,

S. Y.; Tang, C.; Thompson, S.; Parker, J.; Trewin, A.; Bacsa, J.; Slawin, A. M. Z.; Steiner, A.; Cooper, A. I. *Nature Mater.* **2009**, *8*, 973–978.
(57) Bezzu, C. G.; Helliwell, M.; Allan, D. R.; Warren, J. E.; McKeown, N. B. *Science* **2010**, *327*, 1627–1630.
(58) Uribe-Romo, F. J.; Hunt, J. R.; Furukawa, H.; Klock, C.; O'Keeffe, M.; Yaghi, O. M. *J. Am. Chem. Soc.* **2009**, *131*, 4570–4571.
(59) Brunet, P.; Simard, M.; Wuest, J. D. *J. Am. Chem. Soc.* **1997**, *119*, 2737–2738.
(60) Wuest, J. D. *Chem. Commun.* **2005**, 5830–5837.
(61) Chong, J. H.; Ardakani, S. J.; Smith, K. J.; MacLachlan, M. J. *Chem.—Eur. J.* **2009**, *15*, 11824–11828.
(62) Msayib, K.; Walker, J.; McKeown, N. B., unpublished results.
(63) Weber, J.; Su, O.; Antonietti, M.; Thomas, A. *Macromol. Rapid Commun.* **2007**, *28*, 1871–1876.
(64) Ritter, N.; Antonietti, M.; Thomas, A.; Senkovska, I.; Kaskel, S.; Weber, J. *Macromolecules* **2009**, *42*, 8017–8020.
(65) Du, N.; Robertson, G. P.; Pinnau, I.; Thomas, S.; Guiver, M. D. *Macromol. Rapid Commun.* **2009**, *30*, 584–588.
(66) Weber, J.; Antonietti, M.; Thomas, A. *Macromolecules* **2008**, *41*, 2880–2885.
(67) Farha, O. K.; Spokoyny, A. M.; Hauser, B. G.; Bae, Y. S.; Brown, S. E.; Snurr, R. Q.; Mirkin, C. A.; Hupp, J. T. *Chem. Mater.* **2009**, *21*, 3033–3035.
(68) Ghanem, B. S.; Hashem, M.; Harris, K. D. M.; Msayib, K. J.; Xu, M. C.; Budd, P. M.; Chaukura, N.; Book, D.; Tedds, S.; Walton, A.; McKeown, N. B. *Macromolecules* **2010**, 10.1021/ma100640m.
(69) Jiang, J. X.; Su, F.; Niu, H.; Wood, C. D.; Campbell, N. L.; Khimyak, Y. Z.; Cooper, A. I. *Chem. Commun.* **2008**, 486–488.
(70) Jiang, J. X.; Su, F.; Trewin, A.; Wood, C. D.; Campbell, N. L.; Niu, H.; Dickinson, C.; Ganin, A. Y.; Rosseinsky, M. J.; Khimyak, Y. Z.; Cooper, A. I. *Angew. Chem., Int. Ed.* **2007**, *46*, 8574–8578.
(71) Jiang, J. X.; Su, F.; Trewin, A.; Wood, C. D.; Niu, H.; Jones, J. T. A.; Khimyak, Y. Z.; Cooper, A. I. *J. Am. Chem. Soc.* **2008**, *130*, 7710–7720.
(72) Stockel, E.; Wu, X. F.; Trewin, A.; Wood, C. D.; Clowes, R.; Campbell, N. L.; Jones, J. T. A.; Khimyak, Y. Z.; Adams, D. J.; Cooper, A. I. *Chem. Commun.* **2009**, 212–214.
(73) Weber, J.; Thomas, A. *J. Am. Chem. Soc.* **2008**, *130*, 6334–6335.
(74) Jiang, J. X.; Trewin, A.; Su, F. B.; Wood, C. D.; Niu, H. J.; Jones, J. T. A.; Khimyak, Y. Z.; Cooper, A. I. *Macromolecules* **2009**, *42*, 2658–2666.
(75) Schmidt, J.; Werner, M.; Thomas, A. *Macromolecules* **2009**, *42*, 4426–4429.
(76) Cooper, A. I. *Adv. Mater.* **2009**, *21*, 1291–1295.
(77) Zhang, B. F.; Wang, Z. G. *Chem. Commun.* **2009**, 5027–5029.
(78) Kuhn, P.; Forget, A.; Su, D. S.; Thomas, A.; Antonietti, M. *J. Am. Chem. Soc.* **2008**, *130*, 13333–13337.
(79) Kuhn, P.; Thomas, A.; Antonietti, M. *Macromolecules* **2009**, *42*, 319–326.
(80) Ren, H.; Ben, T.; Wang, E. S.; Jing, X. F.; Xue, M.; Liu, B. B.; Cui, Y.; Qiu, S. L.; Zhu, G. S. *Chem. Commun.* **2009**, *46*, 291–293.
(81) Zhang, Y. G.; Riduan, S. N.; Ying, J. Y. *Chem.—Eur. J.* **2009**, *15*, 1077–1081.
(82) Rose, M.; Bohlmann, W.; Sabo, M.; Kaskel, S. *Chem. Commun.* **2008**, 2462–2464.
(83) Webster, O. W.; Gentry, F. P.; Farlee, R. D.; Smart, B. E. *Makromol. Chem., Macromol. Symp.* **1992**, *54/55*, 477.
(84) Webster, O. W.; Gentry, F. P.; Farlee, R. D.; Smart, B. E. *J. Macromol. Sci., Pure Appl. Chem.* **1994**, *A31*, 935–942.
(85) Tilford, R. W.; Mugavero, S. J.; Pellechia, P. J.; Lavigne, J. J. *Adv. Mater.* **2008**, *20*, 2741–2746.
(86) Urraca, J. L.; Carbajo, M. C.; Torralvo, M. J.; Gonzalez-Vazquez, J.; Orellana, G.; Moreno-Bondi, M. C. *Biosens. Bioelectron.* **2008**, *24*, 155–161.
(87) Al Kobaisi, M.; Tate, M.; Rix, C.; Jakubov, T. S.; Mainwaring, D. E. *Adsorption* **2007**, *13*, 315–321.
(88) Farrington, K.; Magner, E.; Regan, F. *Anal. Chim. Acta* **2006**, *566*, 60–68.
(89) O'Mahony, J.; Molinelli, A.; Nolan, K.; Smyth, M. R.; Mizaikoff, B. *Biosens. Bioelectron.* **2006**, *21*, 1383–1392.
(90) Dawson, R.; Laybourn, A.; Clowes, R.; Khimyak, Y. Z.; Adams, D. J.; Cooper, A. I. *Macromolecules* **2009**, *42*, 8809–8816.
(91) Kuhn, P.; Antonietti, M.; Thomas, A. *Angew. Chem., Int. Ed.* **2008**, *47*, 3450–3453.
(92) Ben, T.; Ren, H.; Ma, S. Q.; Cao, D. P.; Lan, J. H.; Jing, X. F.; Wang, W. C.; Xu, J.; Deng, F.; Simmons, J. M.; Qiu, S. L.; Zhu, G. S. *Angew. Chem., Int. Ed.* **2009**, *48*, 9457–9460.
(93) Perret, R.; Ruland, W. *J. Appl. Crystallogr.* **1968**, 308–313.
(94) Suzuki, T.; Miyauchi, M.; Yoshimizu, H.; Tsujita, Y. *Polym. J.* **2001**, *33*, 934–938.
(95) Golemme, G.; Nagy, J. B.; Fonseca, A.; Algieri, C.; Yampolskii, Y. *Polymer* **2003**, *44*, 5039–5045.
(96) Horvath, G.; Kawazoe, K. *J. Chem. Eng. Jpn.* **1983**, *16*, 470–475.
(97) Tao, S. J. *J. Chem. Phys.* **1972**, *56*, 5499–5511.
(98) Eldrup, M.; Lightbody, D.; Sherwood, J. N. *Chem. Phys.* **1981**, *63*, 51–58.
(99) Staiger, C. L.; Pas, S. J.; Hill, A. J.; Cornelius, C. J. *Chem. Mater.* **2008**, *20*, 2606–2608.
(100) Heuchel, M.; Fritsch, D.; Budd, P. M.; McKeown, N. B.; Hofmann, D. *J. Membr. Sci.* **2008**, *318*, 84–99.
(101) Adymkanov, S. V.; Yampol'skii, Y. P.; Polyakov, A. M.; Budd, P. M.; Reynolds, K. J.; McKeown, N. B.; Msayib, K. J. *Polym. Sci., Ser. A* **2008**, *50*, 444–450.
(102) Vandezande, P.; Gevers, L. E. M.; Vankelecom, I. F. J. *Chem. Soc. Rev.* **2008**, *37*, 365–405.
(103) Heinrich, K.; Fritsch, D.; Merten, P.; Dargel, G. S. In International Congress on Membranes and Membrane Processes (ICOM 2008), Hawaii, 2008.
(104) Robeson, L. M. *J. Membr. Sci.* **1991**, *62*, 165–186.
(105) Budd, P. M.; Msayib, K. J.; Tattershall, C. E.; Ghanem, B. S.; Reynolds, K. J.; McKeown, N. B.; Fritsch, D. *J. Membr. Sci.* **2005**, *251*, 263–269.
(106) Robeson, L. M. *J. Membr. Sci.* **2008**, *320*, 390–400.
(107) Budd, P. M.; McKeown, N. B.; Ghanem, B. S.; Msayib, K. J.; Fritsch, D.; Starannikova, L.; Belov, N.; Sanfirova, O.; Yampol'skii, Y. P.; Shantarovich, V. *J. Membr. Sci.* **2008**, *325*, 851–860.
(108) Du, N. Y.; Robertson, G. P.; Song, J. S.; Pinnau, I.; Guiver, M. D. *Macromolecules* **2009**, *42*, 6038–6043.
(109) Du, N. Y.; Robertson, G. P.; Song, J. S.; Pinnau, I.; Thomas, S.; Guiver, M. D. *Macromolecules* **2008**, *41*, 9656–9662.
(110) Du, N. Y.; Robertson, G. P.; Pinnau, I.; Guiver, M. D. *Macromolecules* **2009**, *42*, 6023–6030.
(111) Ahn, J.; Chung, W. J.; Pinnau, I.; Song, J. S.; Du, N. Y.; Robertson, G. P.; Guiver, M. D. *J. Membr. Sci.* **2010**, *346*, 280–287.
(112) Budd, P. M.; Butler, A.; Selbie, J.; Mahmood, K.; McKeown, N. B.; Ghanem, B.; Msayib, K.; Book, D.; Walton, A. *Phys. Chem. Chem. Phys.* **2007**, *9*, 1802–1808.
(113) McKeown, N. B.; Budd, P. M.; Book, D. *Macromol. Rapid Commun.* **2007**, *28*, 995–1002.
(114) Wood, C. D.; Tan, B.; Trewin, A.; Niu, H. J.; Bradshaw, D.; Rosseinsky, M. J.; Khimyak, Y. Z.; Campbell, N. L.; Kirk, R.; Stockel, E.; Cooper, A. I. *Chem. Mater.* **2007**, *19*, 2034–2048.
(115) Han, S. S.; Furukawa, H.; Yaghi, O. M.; Goddard, W. A. *J. Am. Chem. Soc.* **2008**, *130*, 11580–11581.
(116) Makhseed, S.; Samuel, J. *Chem. Commun.* **2008**, 4342–4344.
(117) Makhseed, S.; Samuel, J.; Bumajdad, A.; Hassan, M. *J. Appl. Polym. Sci.* **2008**, *109*, 2591–2597.
(118) Yuan, S. W.; Kirklin, S.; Dorney, B.; Liu, D. J.; Yu, L. P. *Macromolecules* **2009**, *42*, 1554–1559.
(119) Mackintosh, H. J.; Budd, P. M.; McKeown, N. B. *J. Mater. Chem.* **2008**, *18*, 573–578.
(120) Makhseed, S.; Al-Kharafi, F.; Samuel, J.; Ateya, B. *Catal. Commun.* **2009**, *10*, 1284–1287.
(121) Hasell, T.; Wood, C. D.; Clowes, R.; Jones, J. T. A.; Khimyak, Y. Z.; Adams, D. J.; Cooper, A. I. *Chem. Mater.* **2010**, *22*, 557–564.
(122) Rakow, N. A.; Wendland, M. S.; Trend, J. E.; Poirier, R. J.; Paolucci, D. M.; Maki, S. P.; Lyons, C. S.; Swierczek, M. J. *Langmuir* **2010**, *26*, 3767–3770.
(123) Starannikova, L.; Pilipenko, M.; Belov, N.; Yampolskii, Y.; Gringolts, M.; Finkelshtein, E. *J. Membr. Sci.* **2008**, *323*, 134–143.
(124) Finkelshtein, E. S.; Makovetskii, K. L.; Gringolts, M. L.; Rogan, Y. V.; Golenko, T. G.; Starannikova, L. E.; Yampolskii, Y. P.; Shantarovich, V. P.; Suzuki, T. *Macromolecules* **2006**, *39*, 7022–7029.
(125) Alentiev, A. Y.; Yampolskii, Y. P.; Shantarovich, V. P.; Nemser, S. M.; Plate, N. A. *J. Membr. Sci.* **1997**, *126*, 123–132.
(126) Pinnau, I.; Toy, L. G. *J. Membr. Sci.* **1996**, *109*, 125–133.
(127) Nagai, K.; Masuda, T.; Nakagawa, T.; Freeman, B. D.; Pinnau, I. *Prog. Polym. Sci.* **2001**, *26*, 721.

(128) Schmidt, J.; Weber, J.; Epping, J. D.; Antonietti, M.; Thomas, A. *Adv. Mater.* **2009**, *21*, 702-+.
(129) Webster, O. W.; Gentry, F. P.; Farlee, R. D.; Smart, B. E. *Polym. Prepr.* **1991**, *32*, 74–75.
(130) Webster, O. W.; Gentry, F. P.; Farlee, R. D.; Smart, B. E. *Makromol. Chem., Macromol. Symp.* **1992**, *54−5*, 477–482.
(131) Furukawa, H.; Yaghi, O. M. *J. Am. Chem. Soc.* **2009**, *131*, 8875–8883.
(132) Cote, A. P.; El-Kaderi, H. M.; Furukawa, H.; Hunt, J. R.; Yaghi, O. M. *J. Am. Chem. Soc.* **2007**, *129*, 12914–12915.
(133) Wan, S.; Guo, J.; Kim, J.; Ihee, H.; Jiang, D. L. *Angew. Chem., Int. Ed.* **2009**, *48*, 5439–5442.